BCSIR

Available online at www.banglajol.info/index.php/BJSIR

Bangladesh J. Sci. Ind. Res. **60(4)**, 275-286, 2025

BANGLADESH JOURNAL OF SCIENTIFIC AND INDUSTRIAL RESEARCH

ISSN. 0304-9809

Hydraulic and structural analysis of penstock bifurcation with and without sickle plate: Ghar Khola hydropower project, Nepal

R. K. Chaulagain*, R. Thapa and P. Lakhemaru

Department of Automobile and Mechanical Engineering, Thapathali Campus, IOE, TU, Nepal

ARTICLE INFO

Received: 27 July 2025

Revised: 27 August 2025

Accepted: 02 September 2025

eISSN 2224-7157/

DOI: https://doi.org/10.3329/bjsir.v60i4.83047

Abstract

Bifurcation in hydropower plants is essential for directing flow to two turbines, benefiting overall efficiency. The type of bifurcation varies based on site conditions, either symmetric or asymmetric. This study explores asymmetric bifurcation through numerical simulations of multiple models, following hydraulic analysis with and without a sickle plate. Using ANSYS CFX, head loss analysis revealed a flow rate difference of 5 kg/s with a sickle plate and 44 kg/s without. Structural analysis of five models indicated that a combination of a sickle plate and one stiffener is optimal, with an equivalent stress of 120.6 MPa and a safety factor of 2.073. The findings highlight the importance of flow and structural analysis for balanced power generation in double-unit turbines. It recommends further analysis of bifurcation shell thicknesses to enhance design optimization, especially for site-specific applications.

Keywords: Flow analysis; Asymmetric; Structural analysis; Stiffener; Stress; Safety factor

Introduction

The penstock is the water carrier from the height to the turbine in hydropower plants in closed conduit systems (Chaulagain *et al.* 2023). When multiple units of turbines with generators for power generation are designed, multiple penstock lines or branching in multiple numbers are used for several benefits (Dangi *et al.* 2022; Kandel and Luitel, 2019). The branching of penstock pipes in two symmetrical or asymmetrical sections is termed bifurcation and refers to the penstock's Wye (Y-shaped) division to divide flow into two turbine outlets (Flemming *et al.* 2009). In general, the reasons to use bifurcation cover the flow variation, economic, geographical, and maintenance perspectives of the penstock, and the technical specification of the penstock (American Society of Civil Engineers (ASCE), 2012; American Water Works Association (AWWA), 2004; Koirala *et al.* 2017). But, sudden shifting in the direction of flow from the high head causes a transition between the static and dynamic behavior of the flow, and water exhibits irrelevant behavior, such that it receives maximum pressure resting near the powerhouse towards the turbine, as shown in Figure 1, which shows the location. As a result, special considerations for hydraulic losses and structural safety are significant (Dhakal and Shrestha, 2023; Flemming *et al.* 2009).

Several studies have been conducted on bifurcation and identified as a high-pressure component in hydropower plants (Aguirre *et al.* 2019). According to Sukhapure (2017), underground projects have limited bifurcation angles, and unsymmetrical bifurcations can cause geometrical design issues and increased head loss, recommending a bifurcation angle of 30-40° Another research for the symmetrical bifurcation conducted by AHMED S. 1965, showed the head loss coefficient for spherical bifurcations with a higher diameter was 0.44 and 0.30 for the smaller diameter. Similarly,

*Corresponding author's e-mail: rajkrc12@tcioe.edu.np

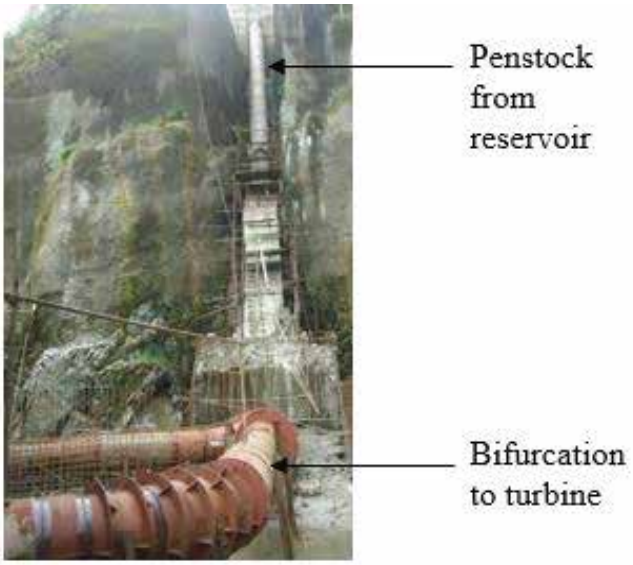

Fig. 1. Location of bifurcation near the power house

the loss coefficient for the taper bifurcation was reported as 0.16 for the 90°C branching and 0.08 to 0.088 for the 60°C branching (Ahmed, 1965).

Penstocks are long cylinders having different wall thicknesses depending on the pressure head on them. Thin-walled unstiffened cylinders, with low buckling resistance, are prone to collapse by asymmetric bifurcation buckling. For a stiffened cylinder, however, external pressure also has the potential to cause the stiffener and thin wall to completely collapse. The thin shell span between two successive stiffeners may collapse, which is known as local collapse if the stiffener resistance is sufficient. Likewise, critical pressure in the cylinder is highly dependent on the nature and magnitude of geometric imperfections such as ovality, weld-induced imperfections, and thickness loss by corrosion. The initial gap existing between steel liners and concrete backfill must be considered in the design of encased steel liners (Jorgen, 2010). Another investigation completed by U. Lasminto (2014) reported that the loss coefficient of a physical model bifurcator decreased with the increasing Reynolds number of inflows. In unsymmetrical bifurcation, the Reynolds number seems higher, concluding a greater head loss coefficient in asymmetrical bifurcation than in symmetrical (Lasminto, 2014). A crescent-shaped rib inside the bifurcation pipe is used to provide strength to the joint known as a sickle or splitter plate, which is resistant to the forces being developed there.

A study conducted by used a CFD and FEM method to optimize a bifurcation of a Kulekhani-III, 14 MW hydropower plant in Nepal and recommended the results for fabrication and installation (Thapa *et al.* 2016). Similarly, Dhakal and Shrestha (2023) concluded that the variation of the taper angle of the cone of bifurcation, the head loss decreases gradually, reaches a minimum, and then increases sharply, while the structural analysis suggested the stiffeners with a safety factor of 1.5. Another study by Neupane and Luintel (2022) analyzed flow for symmetrical and unsymmetrical bifurcation in the ANSYS platform and concluded that the mass flow rate difference from two outlets is minimum for bifurcation of 31°C, such that the head losses are minimal and close for the outlets. A separate research study showed that any objects in static or dynamic loading need to be safe through structural analysis to identify the deflections, stresses, and fatigue life of the same (Daabo *et al.* 2018), and this is followed here for the bifurcation. A design report suggested that the internal and external pressure, impact loads, dead weight of pipe and steel are the major consideration factors on structural analysis specific to the penstock and bifurcation (Department of Electricity Development, 2006). Similarly, research conducted with the use of stiffeners concluded that the bearing capacity of stiffeners and penstock pipe can be suitably modified with the variation in stifferner ring size, cross section, and its quantity (Dong *et al.* 2014), which has been considered in this research for the analysis. The stiffener ring is provided to resist the external load, and it also reduces the equivalent stress developed in the structure. In some pointed sections, induced stress is very high, due to the use of such a ring, which can resist the point load, and finally helps to optimize the thickness of the plate. So, the stiffener is selected by design to make a design suitable with respect to a practical scenario.

From the past reviews conducted, the flow analysis and the structural analysis of asymmetrical bifurcation for the specific case of using a sickle plate and stifferner in combined form were found to have received low attention, though they are of high importance. So, this research covers a flow analysis as well as multiple models for structural analysis, as study taking a case study is used to develop the profile of bifurcation required for the Ghar Khola Hydropower Project of 14 MW, which is the novelty of this research. This combined

form of analysis for a single bifurcation is important and was aimed at the equal distribution of flow on two branches with enough strength among alternatives. The project site is in the Myagdi district of Nepal, with the planned layout of bifurcation as shown in Figure 2, having salient features as listed in Table I. The literature identified that the bifurcation profile depends on site parameters and can be developed by experimental analysis with reduced size or numerical modeling to overcome the complexity of analytical design for calculating head loss. Flow analysis with and without a sickle plate as a research gap is attempted to address within the limitations of the simulation facility available to determine the headloss for the asymmetrical bifurcation model in this research.

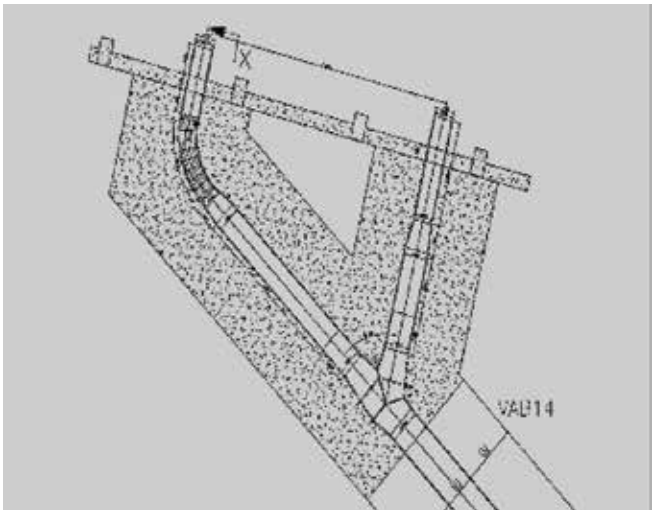

Fig. 2. Layout of the bifurcation installation at the site

without a sickle through hydraulic and structural analysis using the ANSYS platform. For this, methodological steps have been defined as pictured in Figure 3. It summarizes the study as a combined output of hydraulic analysis and structural analysis.

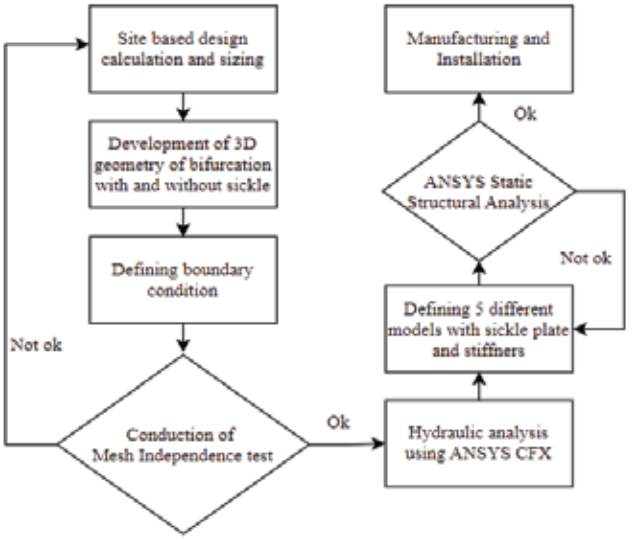

Fig. 3. Flow chart of adopted research methodology

The hydraulic analysis starts with the design of the bifurcation, prepared with the data of the project site based on the guidelines of the Indian Standard (Bureau of Indian Standards, 2009). The design calculation and optimization were done as a result of changing the angle of the bifurcation for minimum head loss. The 3-D geometry for two models with and without a sickle plate was prepared in Solid Works

Table I. Salient features of the project (Nepal Forum, 2024)

Project	Ghar Khola Hydropower Project
Owner	Myagdi Hydropower Limited
Type	Run-of-River (RoR)
Location	Annapurna Rural Municipality 5 and 6, Myagdi District
Plant Capacity	2 x 7 MW, 78.65 GWh
Turbine	Double nozzle, Pelton, 2 units
Design Discharge	3.46 m^3/s
Design head	480.33 m
Total head	604 m (with the addition of 25% surge pressure)
Bifurcation angle	59.5°
Shell thickness	50 mm
Bifurcation axis	Horizontal
Type of bifurcation	Internally reinforced asymmetrical

Materials and methods

The objective of this research is to determine the head loss and strength in a bifurcation of selected sites with and

2018, and a fluid domain was created to import the file into ANSYS CFX. Defining the boundary condition of the fluid domain, a mesh independence test was performed. With satisfaction, the hydraulic analysis with ANSYS CFX was

covered. Furthermore, to conduct the structural analysis, 5 different combinations of sickle and stiffeners were defined and analyzed with ANSYS Static Structural 2018. The selection of one ideal model among the alternatives was the expectation of this research. The selected one was recommended for manufacturing and installation at the site.

Hydraulic simulation and observation

The flow analysis through a pipe under pressure is simple and can be described by one-dimensional and two-dimensional equations precisely. However, the flow near the junction of the branches is difficult and sometimes impossible to describe by a closed-form mathematical solution. In asymmetrical bifurcation, the Reynolds number is high, and the head loss coefficient is a little bit high. ANSYS CFX is used for flow calculation, which is one of the suitable tools for one-directional flow and better stability of results. For the flow analysis, the tetrahedral mesh of the bifurcated model is preferred to identify the maximum velocity and

Fig. 4. Fluid domain of the asymmetrical bifurcation

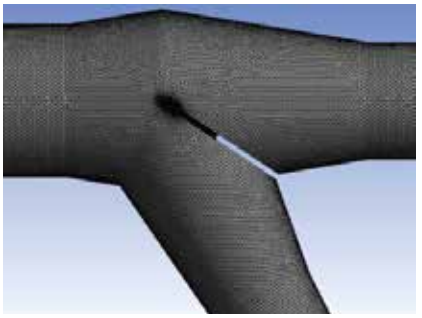

Fig. 5. Fine mesh geometry

recirculation flow rate (Jeong and Seong, 2014) The uniform tetrahedral mesh was prepared for the fluid domain as shown in Figure 4 of asymmetrical bifurcation, and the fine mesh of 5 mm size was made as presented in Figure 5. The mass flow rate was given to the inlet, and the theoretical pressure head was given to the outlet for the boundary condition. The details of the boundary conditions are listed in Table II, in which the dynamic pressure is taken 25% above the normal pressure to manage surge pressure during the operation. Similarly, Table III shows the meshing details that are used in the simulation process.

Table II. Boundary conditions

Boundary conditions	
Inlet	
Mass flow rate	3460 kg/s
Outlet 1 and Outlet 2	
Static Pressure, Normal	4738230 Pa (Normal)
Static Pressure, Dynamic	5922787 Pa (Dynamic)
Wall Features	
Mass and Momentum	No slip wall
Wall roughness	Smooth wall

Table III. Mesh details

Defaults	
Physics Preference	CFD
Solver Preference	CFX
Sizing	
Size function	On Proximity and Curvature
Relevance Center	Fine
No of Element	2880452
Initial Size Seed	Active Assembly
Smoothing	High
Transition	Slow
Span Angle Center	Fine
Inflation	Named Selection
Region of Inflation	Wall
Inflation Criteria	First Layer Thickness (0.0001mm)
Maximum Inflation layer	20
Growth rate	1.2

For numerical simulations of computational fluid dynamics (CFD), the standard k-epsilon (k-ε) model is popularly used, and it seems to perform quite well in determining boundary layer flows (Zhang *et al.* 2017) which is part of Reynolds' Averaged Navier Stokes (RANS) equations. This model provides superior performance for flows that involve rotations, boundary layers under strong adverse pressure gradients, and recirculation. During the simulation, 500 numbers of iterations were done for a fine solution.

The y+ value has been identified by the setting of the first layer thickness of the wall inflation layer. An analytical calculation is carried out to examine the y+ value. Hence, such a value was calculated by using the given known parameters.

Freestream velocity (u) = 3.05950 m/sec
Density of water (ρ) = 1000 kg/m3
Dynamic viscosity (μ) = 0.0000907 kg/ms
Boundary layer length (L) = 1.2 m
Wall distance, first layer thickness (y) = 1x10-6 m
The Reynolds number (Re) is calculated by equation (1).

$$Re = u\ \rho\ L / \mu \quad (1)$$

Calculating, Re = 40478500 was obtained to know the type of flow.

Similarly, the y+ value was calculated by equation (2). The value of y+ is located nearly in front of the sickle plate where the bifurcation starts. When the first layer inflation thickness is 0.0001mm, the y+ value is obtained as 1.1. The variation of the y+ value was obtained as a contour plot in Figure 6.

$$y+ = \frac{y\,\rho\,u}{\mu} \quad (2)$$

Fig. 6. Contour Plot of y+ value

Mesh independence test

A mesh independence (or grid independence) study is something an analyst can perform to determine the dependence of the results on the mesh density. (Kandel and Luitel, 2019b). Mesh independence was done about an output, though it is most often done about stress. However, there are system models that are too coarsely meshed to be adequate for accurate stress output, yet are adequate to capture the stiffness of the structure for accurate deflection or modal frequency output. Table IV shows the results of the mesh independence test till the consistency in head loss depends on the number of elements in the test domain. Figure 7 concluded that the head loss is an increasing number of meshing elements used during the iteration and remains consistent after 1811125 meshing elements. The sensitivity test was conducted with a maximum iteration of 500, with an RMS type of residual targeting 0.00001.

Table IV. Results of mesh independence test

No. of Element	Inlet pressure (Pa)	Pressure loss (Pa)	Head loss (m)
2880452	4744610	11330	1.155
2877123	4744615	11310	1.153
2656230	4745160	9640	0.983
2247851	4745970	7740	0.789
2045756	4747870	6930	0.706
1818452	4749540	6385	0.651
1811125	4749560	6380	0.650

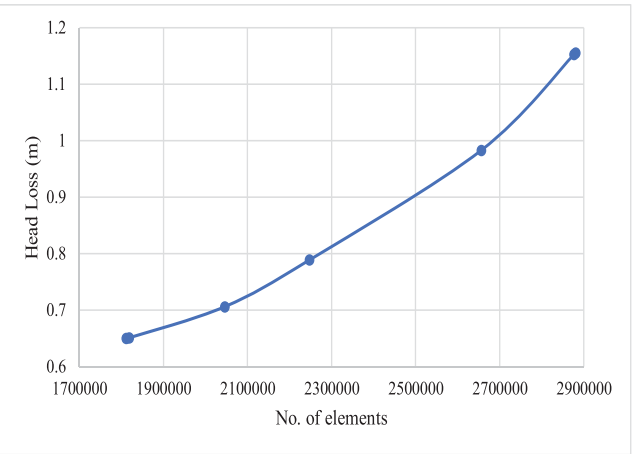

Fig. 7. Variation of head loss with the number of meshing elements

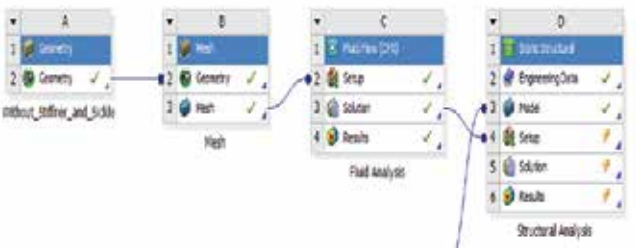

Fig. 8. FSI without a sickle on bifurcation

The aerodynamic load to the structural load was transferred using a Fluid-structure interaction (FSI). By using ANSYS Workbench, the CFD result was "dragged" into the structure project, and the transient and static simulation was performed with the pressure distribution from CFD as pressure loads on the mechanical model. Especially in a system with a surge chamber, valve closing and the subsequent water level oscillation in the surge chamber are the excitation source of the hydraulic transient process. In this system, the result is obtained from the fluid flow analysis as shown in Figure 8.

Flow Behavior

The head loss takes place in a bifurcation due to direction and disturbance in the flow. Whenever there is an obstruction in a pipe, the loss of energy takes place due to a reduction in the area of the cross-section of the pipe at the place where the obstruction is present (Bansal, 2010). There is a sudden enlargement of the area of flow beyond the obstruction, due to which a loss of head takes place.

The loss of head due to obstruction is given by equation (3)

$$h_o = (V_c - V)^2/2g \tag{3}$$

where Vc is the velocity of water at vena contracta and V is the velocity of the liquid in the pipe.

The calculation of head loss due to sudden contraction is given by equation (4)

$$hc = 0.5\, v^2/2g \tag{4}$$

Additionally, the major concern for hydropower developers, the head loss phenomenon, was also considered during the study. The head loss in the system was calculated using Bernoulli's theorem as Equation (5).

$$h_{l_i} = \left(\frac{P_{in}}{\rho * g} + \frac{V_{in}2}{2 * g}\right) - \left(\frac{P_{out_i}}{\rho * g} + \frac{V_{out_i}{}^2}{2 * g}\right) \tag{5}$$

Two models of bifurcation were prepared for fluid flow analysis: one with the sickle plate and the other without a sickle plate. Different behaviors and characteristics of flow were observed under different conditions. Figure 9 shows the pressure experienced by the wall at different zones of asymmetrical bifurcation, being higher in wye branching. The fluctuation of pressure in the bifurcation and further to the penstock is taken as a risk during the safe operation of the plant (Awad and Parrondo, 2023).

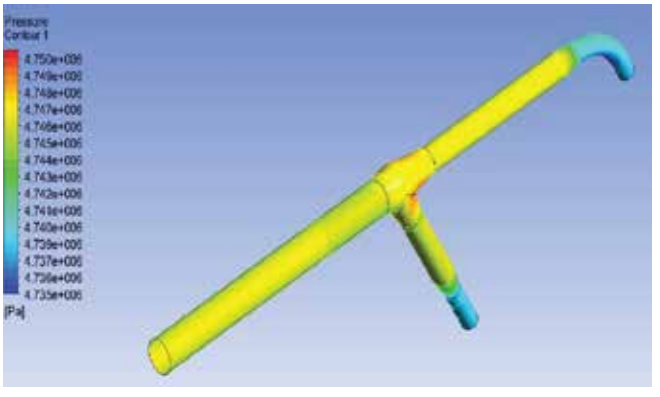

Fig. 9. Pressure distribution at the wall of the bifurcation

Furthermore, the pressure experienced in the sickle zone is shown in Figure 10 and the pressure range inside the bifurcation domain with the sickle is shown in Figure 11. The maximum pressure is observed at the sickle zone.

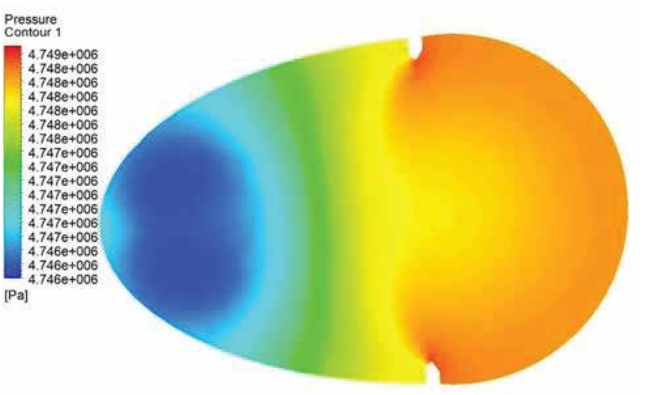

Fig. 10. Pressure at the sickle zone

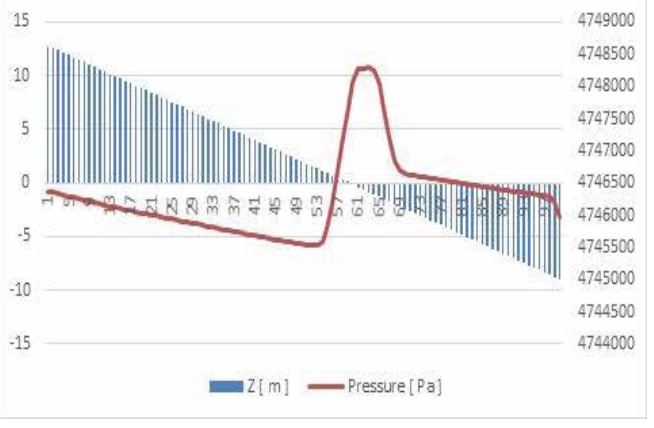

Fig. 11. Pressure range inside the bifurcation

Fig. 12. Velocity streamlines without a sickle in the bifurcation

In bifurcation with a sickle plate, the velocity can be assumed equal in both branches, and head loss is incurred due to the sickle plate. The velocity streamlines on the pipeline without using a sickle plate in the bifurcation are presented in Figure 12, which shows higher velocity at the outlets. Similarly, Figure 13 and Figure 14 show the velocity vector for both models, respectively.

In Figures 13 and 14, the result is presented in a different form of geometrical shape. Generally, the mass flow rate is uneven in the Bifurcation without a sickle plate, as observed in the velocity contour plotted. By comparing the two models, the velocity with the sickle division is found to be 2.78 m/s, which is slightly lower than the case without the sickle plate, having a velocity of 3.16 m/s as the maximum. It is due to the obstruction in the flow because of using the sickle plate, but it balances the amount of flow in the two sections.

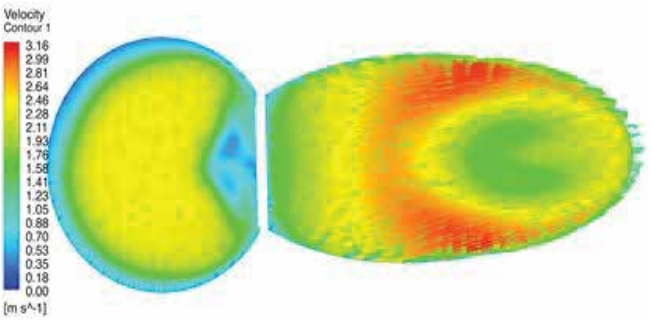

Fig. 13. Velocity vector without sickle plate

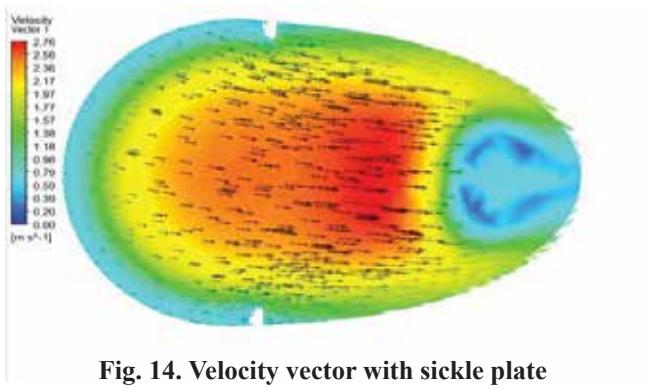

Fig. 14. Velocity vector with sickle plate

Structural simulation and observation

For the structural analysis of the bifurcation, different models were established, which are listed in Table V, and further, a static fluid domain was prepared as presented in Figure 15 to analyze the models.

Table V. Models for structure analysis

Model	Combination of structure
A	Bifurcation shell with sickle and 3 stiffener rings
B	Bifurcation shell without sickle and stiffener ring
C	Bifurcation shell with sickle and only one stiffener
D	Bifurcation shell with only sickle
E	Bifurcation shell of 60 mm thick with only a sickle

The allowable stress of the material is 2/3rd of the yield stress or 1/3 of the ultimate tensile stress, whichever is less (Standard, 1996) The material was taken from IS2062 of Grade E250 or equivalent, with the properties presented in Table VI. For the comparison of plate thickness of plate, the hoop stress was calculated by the formula as per the usual ASME design code. For E250 Material Grading, the allowable stress was calculated to be 137 MPa, which is 1/3rd of the ultimate tensile strength.

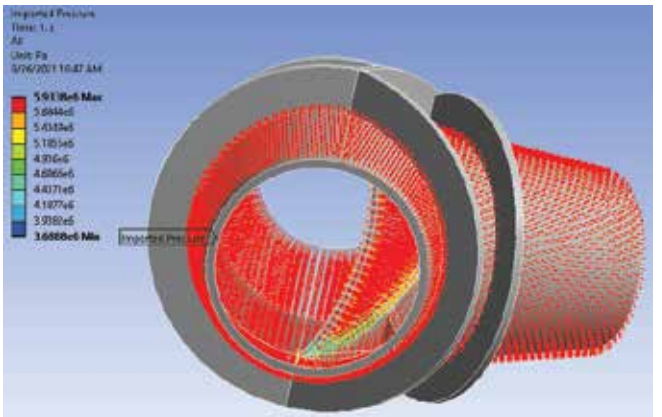

Fig. 15. Fluid domain inserted into the structure

Table VI. Properties of the material IS2062

Parameters	Value
Steel Grade	E250
Density	7850 kg/m^3
Young's modulus	210 GPa
Poisson's Ratio	0.3
Yield Strength	250 MPa
Ultimate tensile strength	410 MPa

For the case of models A, B & C, the total pressure is given for structural analysis. In the case of model D, the maximum stress is developed at the edge of the stiffener ring, whereas the 50 mm sickle is easily permissible for design. Similarly, the comparative design of Model D. Model E is assumed by

mathematical calculation of the same Model D, as the maximum stress is developed at the stiffener area. So, the thickness of the plate is taken at 60 mm for a comparative study of stress analysis. The Von Mises stress and deformation are determined using ANSYS Static Structural 2018.

For maintaining the ovality of the pipe and reducing longitudinal bending stress, a stiffener ring is appropriate. A stiffener ring is used to resist the external pressure in buried regions (Riahi and Showkati, 2009). In general practice, the thickness of the plate is designed a little bit higher by the use of a stiffener ring. The thickness calculation for penstock pipe is given by the relation in the ASME design code, as in equation (6). Stress developed on different models is pictured in Figures 16 to 20.

$$t_{\min} = \frac{P_{total} \times D_i}{2 \times \sigma_{allowable}} \times S \tag{6}$$

where,

Ptotal = Total pressure including static and dynamic head = 604 x 9810 Pa
Di = Inlet Pipe diameter = 1.2 m,
S = Factor of safety

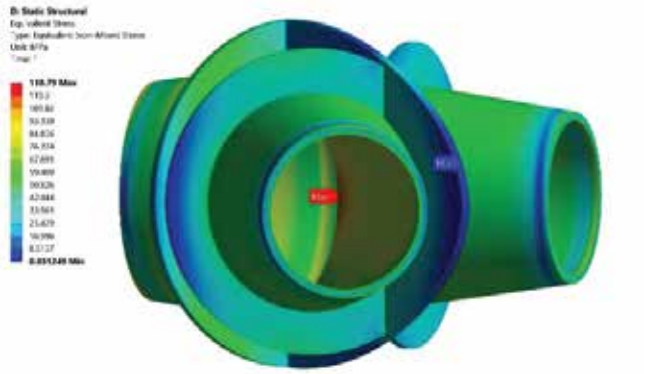

Fig. 16. Equivalent stress of model A

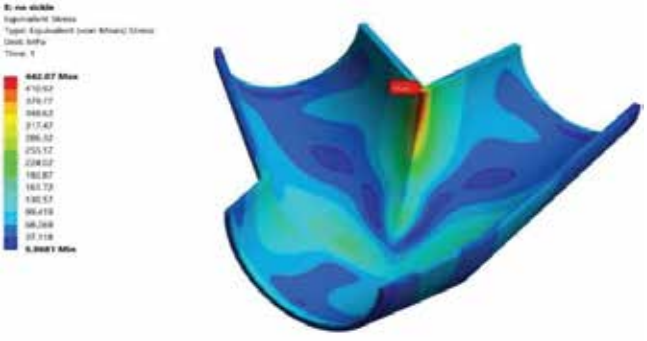

Fig. 17. Equivalent stress of model B

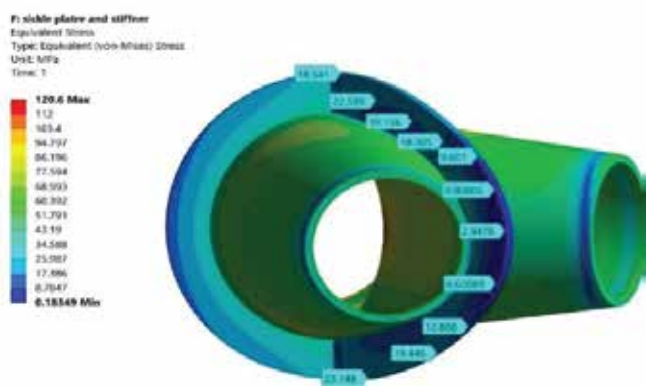

Fig. 18. Equivalent stress of model C

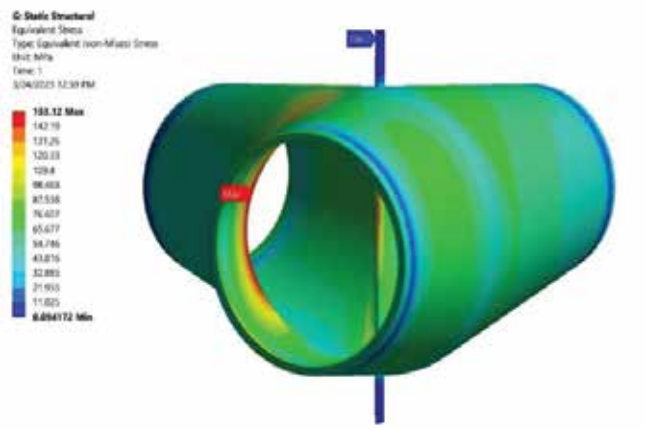

Fig. 19. Equivalent stress of model D

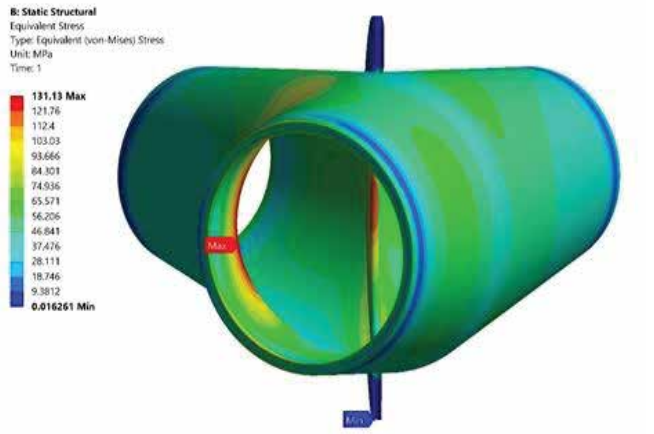

Fig. 20. Equivalent stress of model E

Results and discussion

Since this research has two sections, hydraulic and structural analysis, the results obtained are discussed separately.

Hydraulic analysis

In branches of bifurcation, the discharge is expected to be equal, but with a sickle plate, the velocity decreases, resulting in higher head loss. The head loss and discharge rate calculation at the outlet are found as listed in Table VII for bifurcation with and without a sickle plate.

Table VII. Results of hydraulic analysis

Parameters	Unit	With Sickle	Without Sickle
Head loss	m	0.650	0.380
Mass flow rate on the first branch	kg/sec	1732.39	1752
Mass flow rate on the second branch	kg/sec	1727.61	1708
Head loss coefficient		0.1324	0.062

The head loss and discharge rate analysis were calculated under different conditions. From the result listed in Table 7, the mass flow rate is obtained very close to the actual data in bifurcation with a sickle plate, but the head loss in bifurcation with a sickle plate was found little greater than without a sickle bifurcation. The discharge division at the outlet of the branches was found to be more accurate in the wye, with a sickle of 5 kg/s difference in two branches and a 44 kg/s difference without the sickle. From the hydraulic analysis, it can be concluded that though the use of sickle plates causes some head losses, it plays an important role in dividing the flow equally in branches of the bifurcation and creates a positive impact on power generation.

Structural analysis

After the satisfactory result in hydraulic analysis, the unit is expected to be safe structurally, as well. For the combination of sickle and stiffeners of 5 different models, each model was tested for equivalent stress and deformation. The results obtained are presented in Table VIII.

Table VIII. Summary of structural analysis of different models

Model	Equivalent stress (MPa)	Deformation	Factor of Safety
A	118.79	0.4926	2.105
B	442.07	2.6508	0.566
C	120.6	0.5398	2.073
D	153.12	0.7254	1.633
E	131.13	0.5769	1.934

The head loss in sickle-attached bifurcation is not significant enough to affect energy calculation, but Model B without a sickle is not selected due to unbalanced flow and so high stress concentration. A 3D model of the bifurcation is proposed for the given Model C is suitable for fabrication from an economical point of view. By the use of a sickle plate, the mass flow rate is maintained in such a type of asymmetrical bifurcation, whereas the head loss is not significant. By the use of stiffeners at the upstream side, the thickness of the plate has been minimized and besides, and the downstream stiffener is avoided, resulting in the unnecessary fabrication of stiffeners and the reduction in welding tasks. By comparing Model D with Model E, the maximum stress is observed at the stiffener corner. So, the thickness of the entire bay is increased up to 60 mm instead of a stiffener ring. Finally, the stress observed is 129.25 MPa, which is within the tolerance limit, but the optimization of the plate is not maintained from per economic perspective.

After the stress concentration and deformation, the factor of safety is the next concern, which is the ratio of yield stress to equivalent stress. In the general practice of hydropower design of hydro-mechanical parts, the safety factor is taken as 2 – 3 (Standard, 1996). From the calculation of the safety factor for all the models, the result is presented in Figure 21. It shows that the highest value is for Model A and also possesses the minimum stress, as indicated in Table 8, which is similar to the values for Model C. Based on the limit of safety practices, Model C was selected as the ideal one, rejecting Model A due to its over-design condition. Considering all the concerns discussed and models analyzed, Model C was selected as the final option, which has a factor of safety of 2.073 and an equivalent stress concentration of 120.6 MPa. With a good correlation between numerical models with different scales, the realizable k-epsilon turbulence model meets expectations as a tool for solving problems in scale models, especially in transferring the loss coefficient resulting from a physical model to the loss coefficient of the prototype.

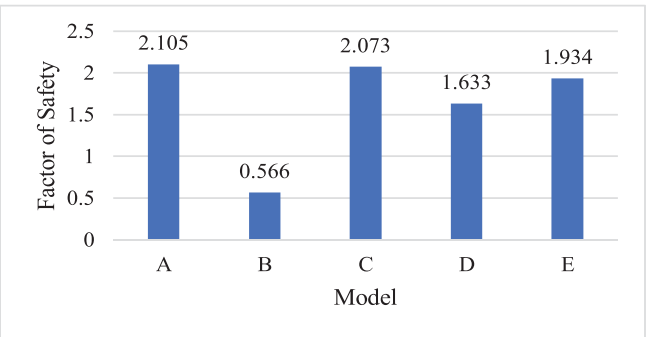

Fig. 21. Factor of safety for different models

Manufacturing and installation

After the optimized result of hydraulic and structural analysis, the detailed drawing was prepared for fabrication and was completed at the site with manufacturing guidelines. Finally, the bifurcation has been installed in the project site as shown in Figures 22 and 23.

Fig. 22. Bifurcation during installation

Fig. 23. Pipeline profile with bifurcation

Conclusion

The objective of determining the flow balance and structurally safe bifurcation through numerical simulation has been achieved using ANSYS CFX and ANSYS Static Structural, respectively. From the hydraulic analysis, the head losses were obtained for asymmetrical bifurcation with and without the sickle plate, resulting in different flows through the branches. The difference in flow rate of 5 kg/s and 44 kg/s with and without using a sickle plate in the bifurcation was calculated. It concludes that though the use of sickle plates causes some head losses, it plays an important role in dividing the flow equally in branches of the bifurcation, creating a balance in power generation. The model possessing the lowest equivalent stress and the highest value of the factor of safety is the ideal from design concerns. To achieve this, the static structural analysis performed among models showed that Model A could fulfill the condition. But compared to Model C, it was felt to be overdesigned due to multiple stiffeners. So, the next Model C was found to be the ideal, considering the cost of multiple stiffeners on Model A and working conditions. It resulted in the equivalent stress concentration of 120.6 MPa and a factor of safety of 2.073, which was the final selection after the structural analysis. From the overall analysis, bifurcation with a sickle plate and only one stiffener has been concluded, fabricated, and installed at the project site. Regarding future recommendations, such simulations are necessary to conduct for site-specific conditions, and furthermore, different thicknesses of bifurcation shells can be analyzed for further optimization in case of asymmetric conditions.

Acknowledgment

The authors are very grateful to Ghar Khola Hydropower Project-14 MW for providing the necessary data and opportunity to permit this research study. Though this research did not receive any financial aid, the different supports received from all of the helping hands who made this research successful are appreciated by the authors.

References

Aguirre CA, Ramirez Camacho RG, de Oliveira W and Avellan F (2019), Numerical analysis for detecting head losses in trifurcations of high head in hydropower plants, *Renewable Energy* **131:** 197–207. https://-doi.org/10.1016/j.renene.2018.07.021

Ahmed S (1965), Head Loss in Symmetrical Bifurcations.

American Society of Civil Engineers (ASCE) (2012), Steel Penstock 2nd Ed. American Society of Civil Engineers. PE John H and Bambei Jr., www.pubs.asce.org

American Water Works Association (AWWA) (2004), Steel Water Pipe : A Guide for Design and Installation. Awwa, Edition, F(C), p 241.

Awad H and Parrondo J (2023), Nonlinear dynamic performance of the turbine inlet valves in hydroelectric power plants. *Advances in Mechanical Engineering,* **15**(1): 1-16. https:// doi.org/ 10.1177/ 168781 3222 1145269

Bansal RK (2010), A text book of Fluid Mechanics and Hydraulic Machines 9th Ed. Laxmi Publications (P) Ltd.

Bureau of Indian Standards (2009), Guidelines for design of branching in penstocks for hydroelectric projects. Bureau of Indian Standards.

Chaulagain RK, Poudel L and Maharjan S (2023), A review on non-conventional hydropower turbines and their selection for ultra-low-head applications, *Heliyon* **9**(7): e17753. https://doi.org/10.1016/j.heliyon.2023.e17753

Daabo AM, Mahmoud S and Al-Dadah RK (2018), Structural analysis of small scale radial turbine for solar powered brayton cycle application. ASME 2018 12th International Conference on Energy Sustainability, ES 2018, Collocated with the ASME 2018 Power Conference and the ASME Nuclear Forum pp 1–10. https://doi.org/10.1115/es2018-7597

Dangi B, Bajracharya TR, Timilsina AB, Chhantyal B and Bista S (2022), Numerical Analysis of Manifold : A Case Study of Phukot Karnali Hydroelectric Project. Proceedings of 11th IOE Graduate Conference, 8914(July), pp 1–8. http://conference.ioe.edu.np/ioegc11/papers/ioegc-11-001-11001.pdf

Department of Electricity Development, G of N (2006), Design guidelines for Water conveyance system of Hydropower Projects. https://www.doed.gov.np/storage/listies/ December2019/ design-guidelines- for-water-conveyance-system.pdf

Dhakal R and Shrestha R (2023), Computational Analysis of Bifurcation of Raghuganga Hydropower Project, *Journal of Advanced College of Engineering and Management (Jacem)* **8**(II): 27–37. https://doi.org/https://doi.org/10.3126/jacem.v8i2.55940

Dong W, Liu X and Li Y (2014), Analysis of stiffened penstock external pressure stability based on immune algorithm and neural network. Mathematical Problems in Engineering. https://doi.org/ 10.1155/ 2014/ 823653

Flemming F, Foust J, Koutnik J and Fisher RK (2009), Overload Surge Investigation Using CFD Data, *International Journal of Fluid Machinery and Systems* **2**(4): 315–323. https:// doi.org/ 10.5293/ijfms.2009.2.4.315

Jeong W and Seong J (2014), Comparison of effects on technical variances of computational fluid dynamics (CFD) software based on finite element and finite volume methods, *International Journal of Mechanical Sciences* **78:** 19–26. https://doi.org/10.1016/j.ijmecsci.2013.10.017

Jorgen A (2010), Buckling and ultimate strength of marine structure.

Kandel B and Luitel MC (2019a), Computational Fluid Dynamics Analysis of Penstock Branching in Hydropower Project, *Journal of Advanced College of Engineering and Management* **5:** 37–43. https://doi.org/10.3126/jacem.v5i0.26676

Kandel B and Luitel MC (2019b), Computational Fluid Dynamics Analysis of Penstock Branching in Hydropower Project, *Journal of Advanced College of Engineering and Management* **5:** 37–43. https://doi.org/10.3126/jacem.v5i0.26676

Koirala R, Chitrakar S, Neopane HP, Chhetri B and Thapa B (2017), Computational design of bifurcation: A case study of darundi khola hydropower project, *International Journal of Fluid Machinery and Systems* **10**(1): 1–8. https://doi.org/10.5293/IJFMS.2017.10.1.001

Lasminto U (2014), Comparative Similarity Study on Hydraulic Losses of a Y-bifurcation. International Symposium on DAMs in a Global Environmnetal Challenges pp 282–291.

Nepal Forum E (2024), Features of Ghar Khola HEP. http://www.nepalenergyforum.com/successfully-complete-the-test-of-gharkhola-hydropower-project-for-cod/

Neupane P and Luintel MC (2022), Flow Analysis in Asymmetric and Symmetric Bifurcation with Varied Layout : A Case Study of Daram Khola HEP. 12th IOE Graduate Conference, October.

Riahi F and Showkati H (2009), Influence of Ring Stiffeners on Ultimate Strength of Submarine Pipelines under Hydro static Pressure. The 9th Asian Pacific Conference on Shell and Spatial Structures.

Standard I (1996), Structural design of penstock -criteria, IS 11639-2. In Bureau of Indian Standards (Vol. 3). https://law.resource.org/pub/in/bis/S14/is.11639.3.1996.pdf

Sukhapure MK, Burns MA, Mahmud MT and Spooner MJ (2017), CFD Modelling and Validation of Pipe Bifurcations. 13th International Conference on Heat Transfer, Fluid Mechanics and Thermodynamics, pp 489–495.

Thapa D, Chandra Luintel M and Ratna Bajracharaya T (2016), Flow Analysis and Structural Design of Penstock Bifurcation of Kulekhani III HEP. IOE Graduate Conference, pp 271–276.

Zhang Z, Wu H, Wang Y, Zhang Q and Li T (2017), Geometrical Design and Hydraulic Feasibility of Inner-Reinforced Girders in Hydropower Bifurcations, *Transactions of Tianjin University* **23**(5): 461–470. https://-doi.org/10.1007/s12209-017-0063-0